

N72.30424

Second Quarterly Report

Design and Control of Remote Manipulators

NASA Contract NAS8-28055

Reporting period 4/5/72 to 7/4/72

This is the second quarterly report on NASA contract NAS8-28055 for Design and Control of Remote Manipulators. The report is divided into five sections:

- I. Summary of technical sections
- II. Vibration modes of manipulators
- III. Optimal path generation
- IV. Studies in control modes and viewing modes
- V. Financial information (included in copies to contractor only)

**CASE FILE
COPY**

I. Summary of Technical Sections

Work proceeded in three main areas during this quarter.


Wayne Book completed the first phase of work on vibrational modes of manipulators, the beginning of which was reported on in the first quarterly report. The main results are

- 1) any arbitrary manipulator may be analyzed for its small motion compliances. From this one may obtain natural frequencies, natural mode amplitudes, and characteristics of free vibration.
- 2) a simulation of the Martin-Marietta shuttle boom proposed configuration, with a 65000 lb. payload attached, indicates three natural frequencies: 1/87 cps, 1/129 cps and 1/357 cps, the first of which dominates in one simulation run made so far.
- 3) the example simulation is for the case of flexible limbs and locked joints. The case of rigid limbs and flexible joints can also be simulated, as well as combinations.

Jan Iemenschot continued his work on determining trajectories for arms so that some integral criterion such as integral of kinetic energy or control torque magnitude is minimized over a motion of the arm. His technique consists of making a series expansion of the torque histories and performing a numerical search for the optimal coefficients in the series. The main result so far is that the optimal coefficients for a wide range of useful motions may be conveniently, although approximately, summarized by a paraboloid which yields the coefficients as functions of the joint angles describing the motion. Thus there is no need to perform the numerical search on line.

Jay Mackro set up equipment and has been performing experiments to evaluate various TV displays in conjunction with manipulator control modes. In particular, the "moving window" has been implemented, although no data on it has been taken. The main result so far is that, for the test task reported, a TV camera mounted directly to the manipulator arm and arranged to look approximately along the arm to the hand allowed the operator to perform the task almost as quickly as he did when viewing the task directly. Worse performance was obtained when viewing through a TV camera fixed to one broad view.

Submitted by


Daniel E. Whitney
Associate Professor

Financial Data

Balance on 6/30/72 (approximately)	\$22,775.00
Expenditures per month anticipated for coming quarter, approximately	1,750.00
Expected balance on October 5, 1972	17, 525.00

Deflection and Vibration of Jointed Beams

Introduction

Manipulator arms are subject to deflection under loads and to vibrations about an equilibrium position when the loading on the arm is suddenly changed. The deflections deteriorate end point accuracy as computed from joint positions and the vibrations can seriously deteriorate the response of the arm, and the ability of an operator to perform desired maneuvers. The following is a method for analyzing the deflection of an arm under given loading conditions. The arm compliance matrix is arrived at giving three displacements and three rotations as a linear function of the applied forces and moments. The method can be used to evaluate the bending of the arm segments and flexible joints as well. If the compliance matrix is nonsingular it can be inverted to yield a spring constant matrix and hence forces and moments as a function of displacements and rotations. The motion of a lumped mass spring system can be described by a linear differential equation using these spring constants. The validity of this approximation for an arm vibrating about an equilibrium position depends largely on how well the mass involved can be lumped into a reasonable number of masses. It is less seriously limited by a small amplitude assumption, the assumption of negligible damping (only second order effects on the natural frequency), and the assumptions that the joint angles are not changing. When the mass of the payload is large compared to the mass of the arm the approximation is very good.

The Mechanics of Arm Deflection

Consider an arm in static equilibrium with the forces and moments on its two ends as is shown in Figure 1. Initially we will assume

- 1) the weight of the arm is negligible
- 2) the arm joints are rigid
- 3) the arm segments are simple beams

When loads are applied to the ends of the arm the individual arm segments deform according to the forces and moments placed on them by the neighboring segments. When these forces are expressed in terms of a coordinate system which has one axis coincident with the neutral axis of the beam as shown in Fig. 2, the deflections over the length of the segment are simply obtained. Each of the deflections and angles along the three mutually perpendicular directions is a linear function of at most two of the loads. Notice that one end of the beam is assumed at the zero position:

$$\Delta X = \alpha_C F_X$$

$$\Delta Y = \alpha_{YF} F_Y + \alpha_{YM} M_Z$$

$$\Delta Z = \alpha_{ZF} F_Z - \alpha_{ZM} M_Y$$

Eq. 1

$$\theta_X = \alpha_{TX} M_X$$

$$\theta_Y = -\alpha_{YF} F_Z + \alpha_{YM} M_Y$$

$$\theta_Z = \alpha_{ZF} F_Y + \alpha_{ZM} M_Z$$

For a beam whose cross section is symmetric about the Y and Z axes $\alpha_{YF} = \alpha_{ZF}$ and will be denoted α_{XF} . This will be the only case specifically considered. The development which follows could retain the extra subscript at some loss in readability. The simplification in notation is as follows:

$$\alpha_{XF} = \alpha_{YF} = \alpha_{ZF}$$

$$\alpha_{XM} = \alpha_{YM} = \alpha_{ZM}$$

$$\alpha_{\theta F} = \alpha_{\theta YF} = \alpha_{\theta ZF}$$

$$\alpha_{\theta M} = \alpha_{\theta YM} = \alpha_{\theta ZM}$$

Beam theory additionally requires that $\alpha_{XM} = \alpha_{\theta F}$. Determining the end displacement is a matter of summing the displacements of the individual segments and in accounting for the displacement due to end point rotations at a distance from the end of the segment where the rotation is calculated. For numerous arbitrary joint angles this becomes a complex bookkeeping task. The matrix procedure which is developed here automatically performs this task.

Transformation of Coordinates Using 4 x 4 Matrices

We are interested in a transformation between two coordinate systems whose origins are displaced from one another and whose axes are not parallel, as in Fig. 3. The position of point P is described in terms of coordinate system 2 by the vector \underline{X}_2 . Given the vector $(\underline{X}_0)_1$ from O_1 to O_2 and the angles between the axes (or lines parallel to them), we desire to find the vector from O_1 to P. This vector is easily found by the following matrix multiplication:

$$\text{Eq. 3} \quad \begin{bmatrix} 1 \\ X_1 \\ Y_1 \\ Z_1 \end{bmatrix} = \begin{bmatrix} 1 & 0 & 0 & 0 \\ (X_0)_1 & \cos(X_2, X_1) & \cos(Y_2, X_1) & \cos(Z_2, X_1) \\ (Y_0)_1 & \cos(X_2, Y_1) & \cos(Y_2, Y_1) & \cos(Z_2, Y_1) \\ (Z_0)_1 & \cos(X_2, Z_1) & \cos(Y_2, Z_1) & \cos(Z_2, Z_1) \end{bmatrix} \begin{bmatrix} 1 \\ X_2 \\ Y_2 \\ Z_2 \end{bmatrix}$$

$$\text{or} \quad \begin{bmatrix} -1 \\ \underline{X}_1 \end{bmatrix} = \begin{bmatrix} 1 & \underline{0}^T \\ (\underline{X}_0)_1 & R_{21} \end{bmatrix} \begin{bmatrix} -1 \\ \underline{X}_2 \end{bmatrix}$$

The cosine terms are the cosines of the angles between intersecting lines parallel to the indicated axes. The sign convention is arbitrary for these angles since the cosine is an even function.

We are interested in coordinate transformations of two special types. One of these is the transformation due to joint angles and displacements.

The other transformation is due to the deflection of arm segments under loading. The former has been described for both rotating and sliding joints by J. Denavit and R. S. Hartenberg (1)* in terms of four independent parameters. The transformation for simple beam flexure, compression, and torsion will be developed in this paper.

Transformation of Coordinates Due to Elastic Deformation

The information we seek is the displacement and rotation of an arm, or more generally a jointed beam, due to the application of loads. The end of the beam can be described in a fixed reference coordinate system if one knows the transformation between the coordinate systems which are fixed to the individual segments. As seen in Fig. 4 the point p at the end of the beam can be described by two transformations, represented by two 4×4 matrices. The transformation A_i relates system i' , the end point before deflection, to system $i-1$. The transformation E_i relates system i to system i' .

$$\text{Eq 4} \quad \begin{bmatrix} 1 \\ \underline{X}_{i', i-1} \end{bmatrix} = A_i E_i \begin{bmatrix} 1 \\ \underline{X}_{i, i} \end{bmatrix} = A_i E_i \begin{bmatrix} 1 \\ \underline{0} \end{bmatrix}$$

where: $\underline{X}_{i, i-1}$ = the position of the origin of system i in terms of system $i-1$

A_i = transformation with no deflection

E_i = transformation due to deflection

$\underline{0}$ = a 3×1 vector whose elements are zero

$\underline{X}_{i, i}$ = location of point p in i coordinates = origin of i in this case

* A reader consulting this paper should be aware of the fact that α_1 in that paper is defined with opposite sign convention of this paper and later papers by Denavit and Hartenberg.

(1) J. Denavit and R. S. Hartenberg; "A Kinematic Notation for Lower-Pair Mechanisms Based on Matrices" Journal of Applied Mechanics June 1955 pp 215-221.

Any number of these transformations may be combined by multiplying the transformation matrices. In terms of the reference system 0, the end of a beam with n joints is located at $\underline{X}_{n,0}$ as is given by:

$$\text{Eq 5} \quad \begin{bmatrix} 1 \\ \underline{X}_{n,0} \end{bmatrix} = A_1 E_1 A_2 \dots A_1 E_1 \dots A_n E_n \begin{bmatrix} 1 \\ 0 \end{bmatrix}$$

We would like the variation of this position vector due to applied forces and moments. First the elements of the E matrices must be found. From Eq 3

$$\text{Eq 6} \quad E_i = \begin{bmatrix} 1 & 0 & 0 & 0 \\ (X_0)_i & \cos(X_i, X_i) & \cos(Y_i, X_i) & \cos(Z_i, X_i) \\ (Y_0)_i & \cos(X_i, Y_i) & \cos(Y_i, Y_i) & \cos(Z_i, Y_i) \\ (Z_0)_i & \cos(X_i, Z_i) & \cos(Y_i, Z_i) & \cos(Z_i, Z_i) \end{bmatrix}$$

For small deflections and small angles the elements of this matrix simplify as follows:

$$\text{Eq 7} \quad E_i = \begin{bmatrix} 1 & 0 & 0 & 0 \\ \Delta X & 1 & \cos(90 + \theta_Z) & \cos(90 - \theta_Y) \\ \Delta Y & \cos(90 - \theta_Z) & 1 & \cos(90 + \theta_X) \\ \Delta Z & \cos(90 + \theta_Y) & \cos(90 - \theta_X) & 1 \end{bmatrix}$$

where θ_X , θ_Y and θ_Z are the angles of rotation about the X, Y and Z axes respectively. For small angles the angles behave very nearly as vectors, thus the order of occurrence is irrelevant. Furthermore the small angle assumption allows further simplification to

$$E_1 = \begin{bmatrix} 1 & 0 & 0 & 0 \\ \Delta X & 1 & -\theta_Z & \theta_Y \\ \Delta Y & \theta_Z & 1 & -\theta_X \\ \Delta Z & -\theta_Y & \theta_X & 1 \end{bmatrix}$$

Eq 8

But these elements were expressed in terms of forces and moments in Eq. 1. Thus E_1 may be expressed as

$$E_1 = \begin{bmatrix} 1 & 0 & 0 & 0 \\ \alpha_{C^F X_{11}} & 1 & -\alpha_{\theta F_1 Y_{11}} - \alpha_{\theta M_1 Z_{11}} & -\alpha_{\theta F_1 Z_{11}} + \alpha_{\theta M_1 Y_{11}} \\ \alpha_{X F_1 Y_{11}} + \alpha_{X M_1 Z_{11}} & \alpha_{\theta F_1 Y_{11}} + \alpha_{\theta M_1 Z_{11}} & 1 & -\alpha_{T_1 M_{X_{11}}} \\ \alpha_{X F_1 Z_{11}} - \alpha_{X M_1 Y_{11}} & \alpha_{\theta F_1 Z_{11}} - \alpha_{\theta M_1 Y_{11}} & \alpha_{T_1 M_{X_{11}}} & 1 \end{bmatrix}$$

Eq 9

where

$F_{X_{11}}, F_{Y_{11}}, F_{Z_{11}}$ = Forces at the end of beam 1, in terms of coordinate system 1

$M_{X_{11}}, M_{Y_{11}}, M_{Z_{11}}$ = Moments at the end of beam 1, in terms of coordinate system 1

Now one must determine the forces and moments on segment 1 which result from the loads on the end of the beam. This is done in the following section:

Equilibrium Forces on the Arm Segments

A free body diagram of the beam segments between coordinate system 1 and system n is shown in Figure 5. Equilibrium requires:

$$\text{Eq 10} \quad \begin{aligned} \text{a) } \sum \underline{F} &= 0 = R_{0i} \underline{F}_{no} - \underline{F}_{-ii} \\ \text{b) } \sum \underline{M}_i &= 0 = R_{0i} \underline{M}_{no} + \underline{r}_{ii} \times R_{0i} \underline{F}_{no} - \underline{M}_{-ii} \end{aligned}$$

- where:
- \underline{F}_{-ii} = the vector from system i to the end of the arm in terms of system i
 - \underline{F}_{-ii} = the force vector acting on the beam to the left of system i in Figure 5, expressed in system i
 - \underline{M}_{-ii} = the moment vector acting on the beam to the left of system i in Figure 5, expressed in system i
 - R_{0i} = 3 x 3 rotation matrix from system 0 to system i
 - \underline{F}_{no} = applied force at the end of segment n, expressed in base coordinate frame
 - \underline{M}_{no} = applied moment expressed in the base frame

Vectorially eq (10) may be expressed as

$$\text{Eq 11} \quad \begin{bmatrix} \underline{F}_{-ii} \\ \underline{M}_{-ii} \end{bmatrix} = \begin{bmatrix} R_{0i} & 0 \\ \underline{r}_{ii} \times R_{0i} & R_{0i} \end{bmatrix} \begin{bmatrix} \underline{F}_{no} \\ \underline{M}_{no} \end{bmatrix}$$

where $\underline{r}_{ii} \times R_{0i}$ may be represented by the matrix multiplication

$$\underline{r}_{ii} \times R_{0i} = \begin{bmatrix} 0 & -r_{zii} & r_{yii} \\ r_{zii} & 0 & -r_{xii} \\ -r_{yii} & r_{xii} & 0 \end{bmatrix} R_{0i}$$

In the above manner we can obtain the forces on the arm segments resulting from the loads on the end of the arm. It remains to evaluate the deflection of the arm by using these values in conjunction with the transformation matrices.

Arm Deflection with Load

Having described the position of the end of the arm (after loading has been placed on the end of the arm) by the coordinate transformation, one could subtract from this vector the vector describing the position of the arm before loading as in equation 13. Theoretically this would be correct.

$$\text{Eq 13} \quad \Delta \underline{X} = \left[(A_1 E_1 A_2 E_2 \dots E_{n-1} A_n E_n) - A_1 A_2 \dots A_n \right] \begin{bmatrix} 1 \\ 0 \end{bmatrix}$$

In practice the difference of these two vectors will be much smaller than the vectors themselves, leading to inaccuracies when the calculation is carried out with two few significant digits. A more practical way is to evaluate the partial derivative of the position of the end with respect to end point loads, for example F_{XNO} and M_{XNO}

$$\text{Eq 14a} \quad \frac{\partial X_{NO}}{\partial F_{XNO}} = \frac{\partial}{\partial F_{XNO}} \left(\begin{bmatrix} A_1 E_1 A_2 E_2 \dots A_n E_n \end{bmatrix} \begin{bmatrix} 1 \\ 0 \end{bmatrix} \right)$$

(read N as
n from here
on)

$$\text{Eq 14b} \quad \frac{\partial X_{NO}}{\partial M_{XNO}} = \frac{\partial}{\partial M_{XNO}} \left(\begin{bmatrix} A_1 E_1 A_2 E_2 \dots A_n E_n \end{bmatrix} \begin{bmatrix} 1 \\ 0 \end{bmatrix} \right)$$

One will now recall the assumption that the joints remain rigid. Because of this:

$$\frac{\partial A_i}{\partial F_{XNO}} = \frac{\partial A_i}{\partial M_{XNO}} = 0 \quad i = 1, 2, \dots, N$$

If one found that this assumption was not valid it would be relatively simple to evaluate these partial derivatives and include joint flexibility.

By the chain rule

$$\text{Eq 16} \quad \frac{\partial X_{-NO}}{\partial F_{XNO}} = A_1 \frac{\partial E_1}{\partial F_{XNO}} A_2 E_2 \dots A_n E_n \left[\frac{1}{0} \right] +$$

$$A_1 E_1 \frac{\partial}{\partial F_{XNO}} (A_2 E_2 \dots A_n E_n) \left[\frac{1}{0} \right]$$

Continuing this differentiation one eventually arrives at: (for example)

$$\text{Eq 17a} \quad \frac{\partial X_{-NO}}{\partial F_{XNO}} = \left\{ \sum_{i=1}^n A_1 E_1 \dots A_i \frac{\partial E_i}{\partial F_{XNO}} A_{i+1} \dots A_n E_n \right\} \left[\frac{1}{0} \right]$$

and similarly for the other force components, as well as for the moments: (for example)

$$\text{Eq 17b} \quad \frac{\partial X_{-NO}}{\partial M_{XNO}} = \left\{ \sum_{i=1}^n A_1 E_1 \dots A_i \frac{\partial E_i}{\partial M_{XNO}} A_{i+1} \dots A_n E_n \right\} \left[\frac{1}{0} \right]$$

Then deflections are obtained as $\Delta_{-NO}^X = \frac{\partial X_{-NO}}{\partial F_{XNO}} \Delta_{XNO}^F$ (17c) for example.

In order to proceed we must evaluate

$$\frac{\partial E_i}{\partial F_{XNO}}, \frac{\partial E_i}{\partial F_{YNO}}, \frac{\partial E_i}{\partial F_{ZNO}}, \frac{\partial E_i}{\partial M_{XNO}}, \frac{\partial E_i}{\partial M_{YNO}}, \text{ and } \frac{\partial E_i}{\partial M_{ZNO}}$$

To do this we take the derivative of the individual elements of Eq. 9 as follows:

Eq 18 $\frac{\partial E_i}{\partial F_{XNO}} =$

0 $\alpha_C \frac{\partial F_{X1i}}{\partial F_{XNO}}$ $\alpha_{XF1} \frac{\partial F_{Y1i}}{\partial F_{XNO}} + \alpha_{XMI} \frac{\partial M_{Z1i}}{\partial F_{XNO}}$ $\alpha_{XF1} \frac{\partial F_{Z1i}}{\partial F_{XNO}} - \alpha_{XMI} \frac{\partial M_{Y1i}}{\partial F_{XNO}}$	0 0 $\alpha_{\theta F1} \frac{\partial F_{Y1i}}{\partial F_{XNO}} + \alpha_{\theta MI} \frac{\partial M_{Z1i}}{\partial F_{XNO}}$ $\alpha_{\theta F1} \frac{\partial F_{Z1i}}{\partial F_{XNO}} - \alpha_{\theta MI} \frac{\partial M_{Y1i}}{\partial F_{XNO}}$	0 0 0 $\alpha_T \frac{\partial F_{X1i}}{\partial F_{XNO}}$
--	---	--

Similarly for F_{YNO} , F_{ZNO} , M_{XNO} , M_{YNO} , and M_{ZNO} . Note that the derivative of the rotation submatrix is antisymmetric

There is but one thing left to evaluate, that is

$$\frac{\partial F_{-1i}}{\partial F_{-NO}}, \frac{\partial F_{-1i}}{\partial M_{-NO}}, \frac{\partial M_{-1i}}{\partial F_{-NO}}, \text{ and } \frac{\partial M_{-1i}}{\partial M_{-NO}}. \text{ Referring to Eq 11}$$

it is seen that these partial derivatives are readily evaluated if one assumes that R_{0i} and $\underline{r}_{1i} \times R_{0i}$ are essentially independent of the loading, which they are to first order. Then

Eq 19
$$\frac{\partial}{\partial F_{XNO}} \begin{bmatrix} F_{-1i} \\ M_{-1i} \end{bmatrix} = \left[\begin{array}{c|c} R_{0i} & 0 \\ \hline \underline{r}_{1i} \times R_{0i} & R_{0i} \end{array} \right] \begin{bmatrix} 1 \\ 0 \\ 0 \\ 0 \\ 0 \\ 0 \end{bmatrix}$$

In general

$$\text{Eq 20} \quad \begin{bmatrix} F_{-ii} \\ M_{-ii} \end{bmatrix} \begin{bmatrix} \frac{\partial}{\partial F_{XNO}} & \frac{\partial}{\partial F_{YNO}} & \frac{\partial}{\partial F_{ZNO}} & \frac{\partial}{\partial M_{XNO}} & \frac{\partial}{\partial M_{YNO}} & \frac{\partial}{\partial M_{ZNO}} \end{bmatrix} =$$

$$\begin{bmatrix} R_{O1} & | & 0 \\ \hline F_{-ii} \times R_{O1} & | & R_{O1} \end{bmatrix}$$

These values can be substituted into Equation 18 to yield the derivative of the elastic deflection transformation matrix with respect to the end of arm loads. It has already been pointed out how the displacements are computed using these transformations. The next section will show how to arrive at the rotation of the end of the arm due to the loads.

End Point Rotations Under Loads

If one carries out the summation enclosed in the braces in Eq. 17 for all six components of forces and moments, the result will be a 4 x 4 matrix to be multiplied by a vector. If the loads are applied at the end of the arm, the vector is $[1 \ 0 \ 0 \ 0]^T$. If however, the arm extends past the point of application of the loads, the vector will be $[1 \ X'_{NN} \ Y'_{NN} \ Z'_{NN}]^T$. We can interpret the elements of the 4 x 4 matrix in the following manner:

$$\text{Eq 21} \quad \frac{\partial \underline{X}_{NO}}{\partial F_{XNO}} = \begin{bmatrix} 0 & 0 & 0 & 0 \\ \delta X_{NO} & \frac{\partial^2 X_{NO}}{\partial X'_{NN} \partial F_{XNO}} & \frac{\partial^2 X_{NO}}{\partial Y'_{NN} \partial F_{XNO}} & \frac{\partial^2 X_{NO}}{\partial Z'_{NN} \partial F_{XNO}} \\ \delta Y_{NO} & \frac{\partial^2 Y_{NO}}{\partial X'_{NN} \partial F_{XNO}} & \frac{\partial^2 Y_{NO}}{\partial Y'_{NN} \partial F_{XNO}} & \frac{\partial^2 Y_{NO}}{\partial Z'_{NN} \partial F_{XNO}} \\ \delta Z_{NO} & \frac{\partial^2 Z_{NO}}{\partial X'_{NN} \partial F_{XNO}} & \frac{\partial^2 Z_{NO}}{\partial Y'_{NN} \partial F_{XNO}} & \frac{\partial^2 Z_{NO}}{\partial Z'_{NN} \partial F_{XNO}} \end{bmatrix} \begin{bmatrix} 1 \\ \Delta X'_{NN} \\ \Delta Y'_{NN} \\ \Delta Z'_{NN} \end{bmatrix}$$

Which we will denote as

$$\text{Eq 22} \quad \frac{\partial \underline{X}_{NO}}{\partial F_{XNO}} = \begin{bmatrix} 0 & \underline{0} \\ \delta X_{NO} & \delta R_{NN} \end{bmatrix} \begin{bmatrix} 1 \\ \underline{\Delta X'_{NN}} \end{bmatrix}$$

Here δX_{NO} , δY_{NO} , δZ_{NO} are the displacements of the origin of coordinate system N. δR_{NN} is the lower right 3 x 3 submatrix of Eq 21. The first subscript refers to the point, and the second subscript refers to the orientation of the vector $[1 \ \Delta X'_{NN} \ \Delta Y'_{NN} \ \Delta Z'_{NN}]$.

Equation 22 can also be written in the following form, using a transformation of coordinates.

$$\text{Eq 23} \quad \frac{\partial \underline{X}_{NO}}{\partial F_{XNO}} = \begin{bmatrix} 0 & \underline{0} \\ \delta X_{NO} & \delta R_{NO} \end{bmatrix} \begin{bmatrix} 1 & \underline{0} \\ \underline{0} & R_{ON} \end{bmatrix} \begin{bmatrix} 1 \\ \underline{\Delta X'_{NO}} \end{bmatrix}$$

On multiplying together the two 4 x 4 matrices one obtains:

$$\text{Eq 24} \quad \frac{\partial \underline{X}_{NO}}{\partial F_{XNO}} = \begin{bmatrix} 0 & \underline{0} \\ \delta X_{NO} & \delta R_{N \ R_{ON}} \end{bmatrix} \begin{bmatrix} 1 \\ \underline{\Delta X'_{NO}} \end{bmatrix}$$

which we denote as:

$$\text{Eq 25} \quad \frac{\partial X_{NO}}{\partial F_{XNO}} = \left[\begin{array}{c|c} 0 & 0 \\ \hline \delta X_{NO} & \delta R_{NO} \end{array} \right] \left[\begin{array}{c} 1 \\ \Delta X'_{NO} \end{array} \right]$$

Now look at the physical situation as portrayed in Fig. 6, a view of the arm's end parallel to the Z_0 axis. The way in which the deflection of the end point changes if that end point is extended beyond the load depends only on the rotation and the extension. Thus we can interpret the δR_{NO} matrix as follows:

$$\text{Eq 26} \quad \delta R_{NO} = \delta R_{NN} R_{ON} = \left[\begin{array}{ccc} 0 & -\delta\theta_{ZNO} & \delta\theta_{YNO} \\ \delta\theta_{ZNO} & 0 & -\delta\theta_{XNO} \\ -\delta\theta_{YNO} & \delta\theta_{XNO} & 0 \end{array} \right]$$

where $\delta\theta_{ZNO} = \frac{\partial\theta_{ZNO}}{\partial F_{XNO}}$
 $\delta\theta_{XNO} = \frac{\partial\theta_{XNO}}{\partial F_{XNO}}$ etc.

In this case $\frac{\partial}{\partial F_{XNO}}$ was used. Similarly of course one can obtain the partial derivatives with respect to the other loads.

Compliance Matrix and Spring Constant Matrix

Now we are able to piece together the above derivation to reach our original goal: a matrix of compliance of the arm under force. Equations 16, 17 and 26 are evaluated (as well as the similar equations for the other forces and moments) and one can construct the following matrix equation.

Eq 27a)

$$\begin{bmatrix} \Delta X \\ \Delta Y \\ \Delta Z \\ \Delta \theta_X \\ \Delta \theta_Y \\ \Delta \theta_Z \end{bmatrix} = \begin{bmatrix} \frac{\partial X}{\partial F_X} & \frac{\partial X}{\partial F_Y} & \frac{\partial X}{\partial F_Z} & \frac{\partial X}{\partial M_X} & \frac{\partial X}{\partial M_Y} & \frac{\partial X}{\partial M_Z} \\ \frac{\partial Y}{\partial F_X} & \frac{\partial Y}{\partial F_Y} & \frac{\partial Y}{\partial F_Z} & \frac{\partial Y}{\partial M_X} & \frac{\partial Y}{\partial M_Y} & \frac{\partial Y}{\partial M_Z} \\ \frac{\partial Z}{\partial F_X} & \frac{\partial Z}{\partial F_Y} & \frac{\partial Z}{\partial F_Z} & \frac{\partial Z}{\partial M_X} & \frac{\partial Z}{\partial M_Y} & \frac{\partial Z}{\partial M_Z} \\ \frac{\partial \theta_X}{\partial F_X} & \frac{\partial \theta_X}{\partial F_Y} & \frac{\partial \theta_X}{\partial F_Z} & \frac{\partial \theta_X}{\partial M_X} & \frac{\partial \theta_X}{\partial M_Y} & \frac{\partial \theta_X}{\partial M_Z} \\ \frac{\partial \theta_Y}{\partial F_X} & \frac{\partial \theta_Y}{\partial F_Y} & \frac{\partial \theta_Y}{\partial F_Z} & \frac{\partial \theta_Y}{\partial M_X} & \frac{\partial \theta_Y}{\partial M_Y} & \frac{\partial \theta_Y}{\partial M_Z} \\ \frac{\partial \theta_Z}{\partial F_X} & \frac{\partial \theta_Z}{\partial F_Y} & \frac{\partial \theta_Z}{\partial F_Z} & \frac{\partial \theta_Z}{\partial M_X} & \frac{\partial \theta_Z}{\partial M_Y} & \frac{\partial \theta_Z}{\partial M_Z} \end{bmatrix} \begin{bmatrix} F_X \\ F_Y \\ F_Z \\ M_X \\ M_Y \\ M_Z \end{bmatrix}$$

NO NO NO

or

Eq 27b)

$$\begin{bmatrix} \Delta \underline{X} \\ \Delta \underline{\theta} \end{bmatrix} = \underset{\text{NO}}{C} \begin{bmatrix} \underline{F} \\ \underline{M} \end{bmatrix} \underset{\text{NO}}{}$$

The subscripts on the matrices are understood to apply to each element. Due to the nature of the problem the matrix C_{NO} will be symmetric. The inverse of the matrix C_{NO} will be the spring constant matrix K_{NO} and

$$\text{Eq 28} \quad \begin{bmatrix} \underline{F} \\ \underline{M} \end{bmatrix}_{\text{NO}} = C_{\text{NO}}^{-1} \begin{bmatrix} \underline{\Delta X} \\ \underline{\Delta \theta} \end{bmatrix}_{\text{NO}} = K_{\text{NO}} \begin{bmatrix} \underline{\Delta X} \\ \underline{\Delta \theta} \end{bmatrix}_{\text{NO}}$$

C_{NO} will nonsingular for all physical cases. For some arm configurations and parameters the inverse may require excessive accuracy, and hence be uncalculable. In this case one must eliminate one or more of the directions from consideration to get an invertible matrix.

Linear Beam Vibrations

Up until this point we have been considering the displacements of and loads on a static beam. If one considers a rigid mass with inertia placed at the loading point, the forces and moments on that mass are the negative of the forces and moments on the beam. These forces and moments can be determined from the spring constant matrix and the deviation of the mass from the equilibrium position. Since structural damping is small, the natural frequency of the spring-mass system as well as the amplitude ratios of the various modes of vibration can be determined. Nonlinearities such as Coriolis accelerations and centripetal accelerations can be neglected for angular velocities which are appropriately small. This seems to be the case in practical arm problems with small vibrations. The equations of motion are then written as

$$\text{Eq 29} \quad \begin{bmatrix} M & 0 & 0 & 0 & 0 & 0 \\ 0 & M & 0 & 0 & 0 & 0 \\ 0 & 0 & M & 0 & 0 & 0 \\ 0 & 0 & 0 & I_{XX} & I_{XY} & I_{XZ} \\ 0 & 0 & 0 & I_{XY} & I_{YY} & I_{YZ} \\ 0 & 0 & 0 & I_{XZ} & I_{YZ} & I_{ZZ} \end{bmatrix} \frac{d^2}{dt^2} \begin{bmatrix} \underline{\Delta X} \\ \underline{\Delta \theta} \end{bmatrix}_{\text{NO}} = -K_{\text{NO}} \begin{bmatrix} \underline{\Delta X} \\ \underline{\Delta \theta} \end{bmatrix}_{\text{NO}}$$

where: M = the lumped mass at the end of the arm

I_{XX}, I_{YY}, I_{ZZ} = the mass moments of inertia of the lumped inertia at the end of the arm about axes parallel to the reference axes but through the center of mass.

I_{XY}, I_{XZ}, I_{YZ} = the cross moments of inertia about axes parallel to the reference axes but through the center of mass.

for convenience Eq 29 will be rewritten as

$$J_{NO} \frac{d^2}{dt^2} \begin{bmatrix} \Delta \underline{X} \\ \Delta \underline{\theta} \end{bmatrix} = -K_{NO} \begin{bmatrix} \Delta \underline{X} \\ \Delta \underline{\theta} \end{bmatrix}$$

NO

This can be written in state variable form as

$$\text{Eq 31} \quad \frac{d}{dt} \begin{bmatrix} \Delta \underline{X} \\ \Delta \underline{\theta} \\ \Delta \dot{\underline{X}} \\ \Delta \dot{\underline{\theta}} \end{bmatrix} = \begin{bmatrix} 0 & I \\ -J^{-1} K & 0 \end{bmatrix} \begin{bmatrix} \Delta \underline{X} \\ \Delta \underline{\theta} \\ \Delta \dot{\underline{X}} \\ \Delta \dot{\underline{\theta}} \end{bmatrix} = A \begin{bmatrix} \Delta \underline{X} \\ \Delta \underline{\theta} \\ \Delta \dot{\underline{X}} \\ \Delta \dot{\underline{\theta}} \end{bmatrix}$$

The dot above $\Delta \underline{X}$ and $\Delta \underline{\theta}$ indicate a derivative with respect to time. The roots of the equation

$$\text{Eq 32} \quad |sI - A| = 0$$

are the natural frequencies of the system. The amplitude ratios can be found as for any undamped linear system.

Extensions - More Than One Lumped Mass

The case of the unloaded or lightly loaded arm is one in which the dynamics of the arm vibration are not dominated by one lumped mass. The criteria for modeling with lumped masses will not be discussed here, but rather the use of the technique developed will be extended to include any number of lumped masses. Figure 7 shows schematically a model that one may be interested in.

Initially one obtains spring constants between each mass point and its adjacent mass points. The nonequilibrium forces on each mass depend only on the difference in the vector positions of it and its neighbors. Thus for the example in Figure 7, with some change in notation:

$$\text{Eq 33} \quad J_i \ddot{\underline{X}}_i = K_{i, i-1} (\underline{X}_{i-1} - \underline{X}_i) + K_{i+1, i} (\underline{X}_{i+1} - \underline{X}_i)$$

where $\underline{X}_i = \begin{bmatrix} \underline{\Delta X} \\ \underline{\Delta \theta} \end{bmatrix}_i$ = position and angular orientation for mass i, measured from equilibrium in base coordinates

$K_{i, i-1}$ = spring constant matrix between mass i and mass i-1

$K_{i+1, i}$ = spring constant matrix between mass i and mass i+1

J_i = the inertia matrix for mass i

This equation can be written for all n masses. The end masses are special cases

$$\text{Eq 34} \quad J_1 \ddot{\underline{X}}_1 = -K_{10} \underline{X}_1 + K_{21} (\underline{X}_2 - \underline{X}_1)$$

$$\text{Eq 35} \quad J_N \ddot{\underline{X}}_N = K_{N, N-1} (\underline{X}_{N-1} - \underline{X}_N)$$

is similar to the large matrix in Eq 36, but the J^{-1} terms are removed. Then

$$\text{Eq 37} \quad \underline{C} = \underline{K}^{-1}$$

$$\begin{bmatrix} \underline{x} \\ \underline{\Theta} \end{bmatrix} = \underline{C} \begin{bmatrix} \underline{F} \\ \underline{M} \end{bmatrix}$$

where \underline{F} = unknown, possibly nonzero loading
 \underline{x} = displacements or angles associated with the \underline{F} elements
 \underline{M} = loading terms which will be identically zero
 $\underline{\Theta}$ = angles associated with the \underline{M} elements

$$\text{Eq 39} \quad \begin{bmatrix} \underline{x} \\ \underline{\Theta} \end{bmatrix} = \underline{C} \begin{bmatrix} \underline{F} \\ \underline{0} \end{bmatrix} = \begin{bmatrix} c_{11} & c_{12} \\ c_{21} & c_{22} \end{bmatrix} \begin{bmatrix} \underline{F} \\ \underline{0} \end{bmatrix}$$

$$\text{Eq 40} \quad \underline{x} = c_{11} \underline{F}$$

$$\text{Eq 41} \quad \underline{\Theta} = c_{21} \underline{F}$$

$$\text{Eq 42} \quad \begin{bmatrix} \underline{F} \\ \underline{0} \end{bmatrix} = \underline{K} \begin{bmatrix} \underline{x} \\ \underline{\Theta} \end{bmatrix} = \underline{K} \begin{bmatrix} \underline{x} \\ c_{21} \underline{F} \end{bmatrix}$$

$$\text{Eq 43} \quad = \begin{bmatrix} k_{11} & k_{12} \\ k_{21} & k_{22} \end{bmatrix} \begin{bmatrix} \underline{x} \\ c_{21} \underline{F} \end{bmatrix}$$

$$\text{Eq 44} \quad \underline{F} = \kappa_{11} \underline{x} + \kappa_{12} \underline{C}_{21} \underline{F}$$

$$\text{Eq 45} \quad \underline{F} = (I - \kappa_{12} \underline{C}_{21})^{-1} \kappa_{11} \underline{x}$$

The above operations assume the inverse can be performed.

The reduced equations of motion are then:

$$\text{Eq 46} \quad \mathcal{M} \frac{d^2}{dt^2} \underline{x} = (I - \kappa_{12} \underline{C}_{21})^{-1} \kappa_{11} \underline{x}$$

where \mathcal{M} is the reduced inertia matrix obtained by eliminating the appropriate rows and columns from the unreduced inertia matrix.

Example Problem

In order to verify and illustrate the feasibility of the theory presented above, a computer program was developed to evaluate the coefficient matrix for an example arm. The coefficient matrix was then input to an existing matrix manipulation program along with an inertia matrix to develop the equations of motion for a simple case.

As a realistic example the arm parameters and configuration were taken from a proposal by the Martin Marietta Company for a boom for the space shuttle. These are shown in Table 1. Figure 8 shows the arm in the configuration of the example and the distribution of the 65,000 lb. load. These joint angles were chosen because they realistically duplicate a position in a retrieve maneuver for which the arm might be used. It also enables a separation of modes reducing the number of state variables to six. This is due to the planar motion of the mass. Figure 9 indicates the oscillations resulting from an initial displacement of ten inches in the Y direction at the endpoint.

The computer program required 0.08 hours of IBM 1130 computer time to evaluate the compliance matrix for six joint angle positions. This includes some compilation and program listing time, and the program could be considerably streamlined.

Future Work

Preliminary work has developed the controllability matrix for the general case with joint angle position control. This has been used to show that the example problem above is controllable using two of the joints. Optimal control theory can now be used to determine suitable feedback gains if one has access to the state variables. The state variables can be partially measured and partially reconstructed using the measured variables. Measurements might be performed via accelerometers, optically, or in some other fashion. In all this future work the method developed here will make the determination of the equations of motion for arm vibration practical, even for complicated arm configurations.

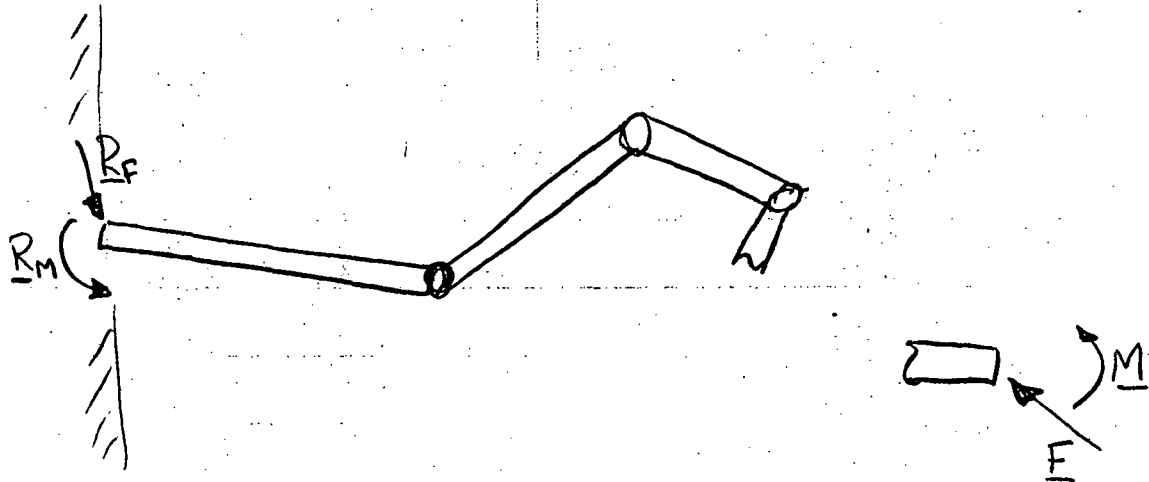


Fig. 1 A multi jointed arm in equilibrium between the applied loads \underline{F} and \underline{M} and the reactions \underline{R}_F and \underline{R}_m

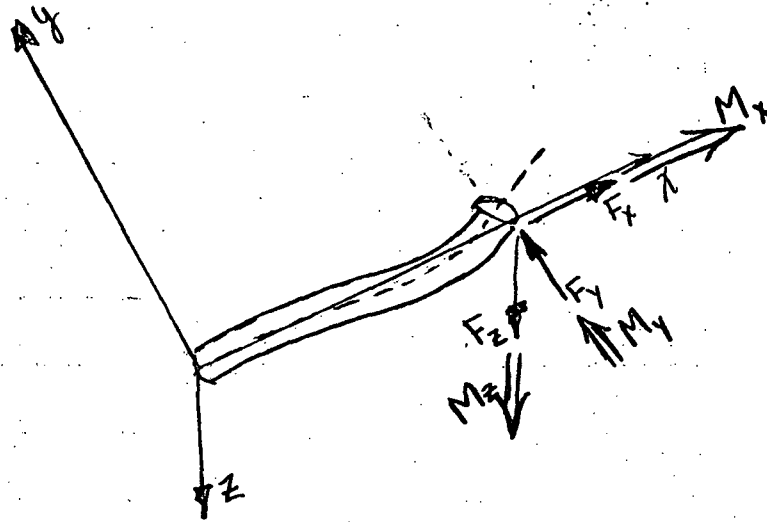


Fig. 2 A coordinate system oriented with respect to an arm segment.

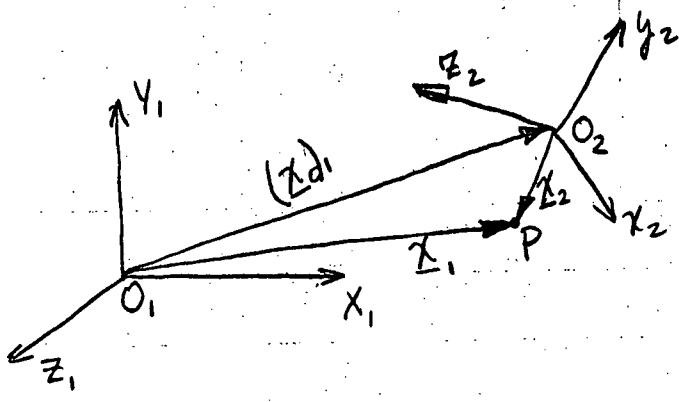


Fig. 3 A transformation between coordinates .

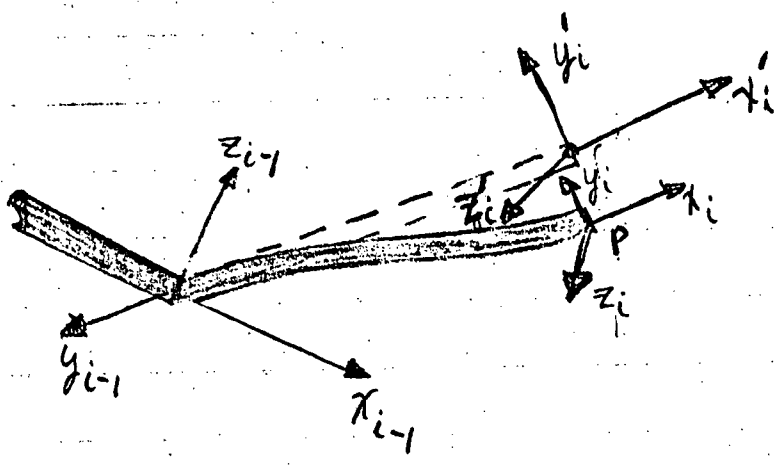


Fig. 4 Transformations in a deformed and undeformed beam .

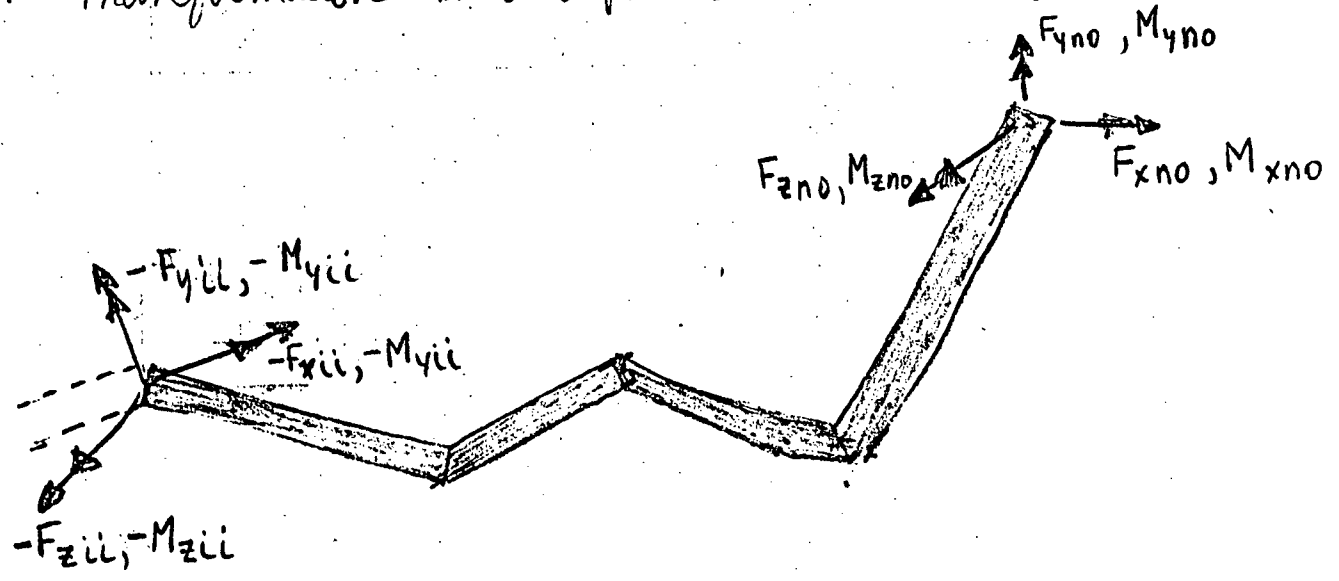


Fig 5. Free body diagram of a portion of the arm in equilibrium

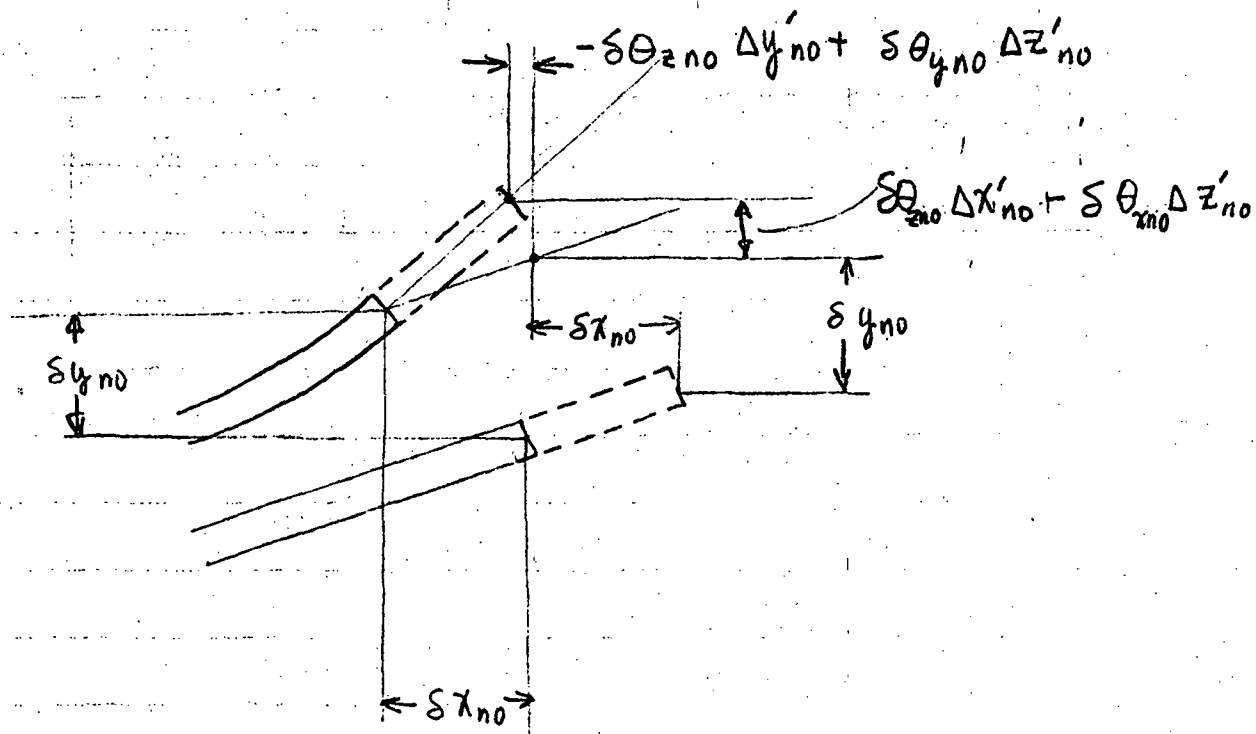


Fig. 6. Interpreting the rotation of the endpoint.

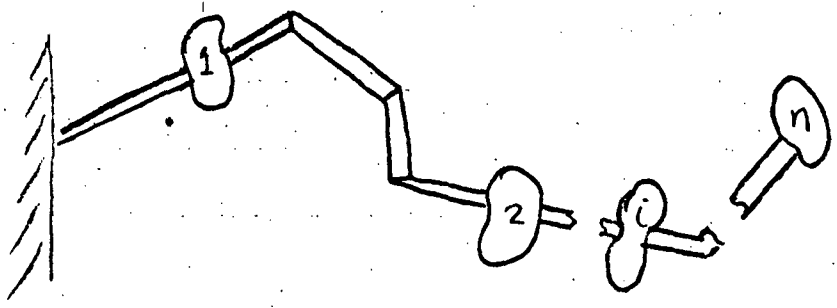
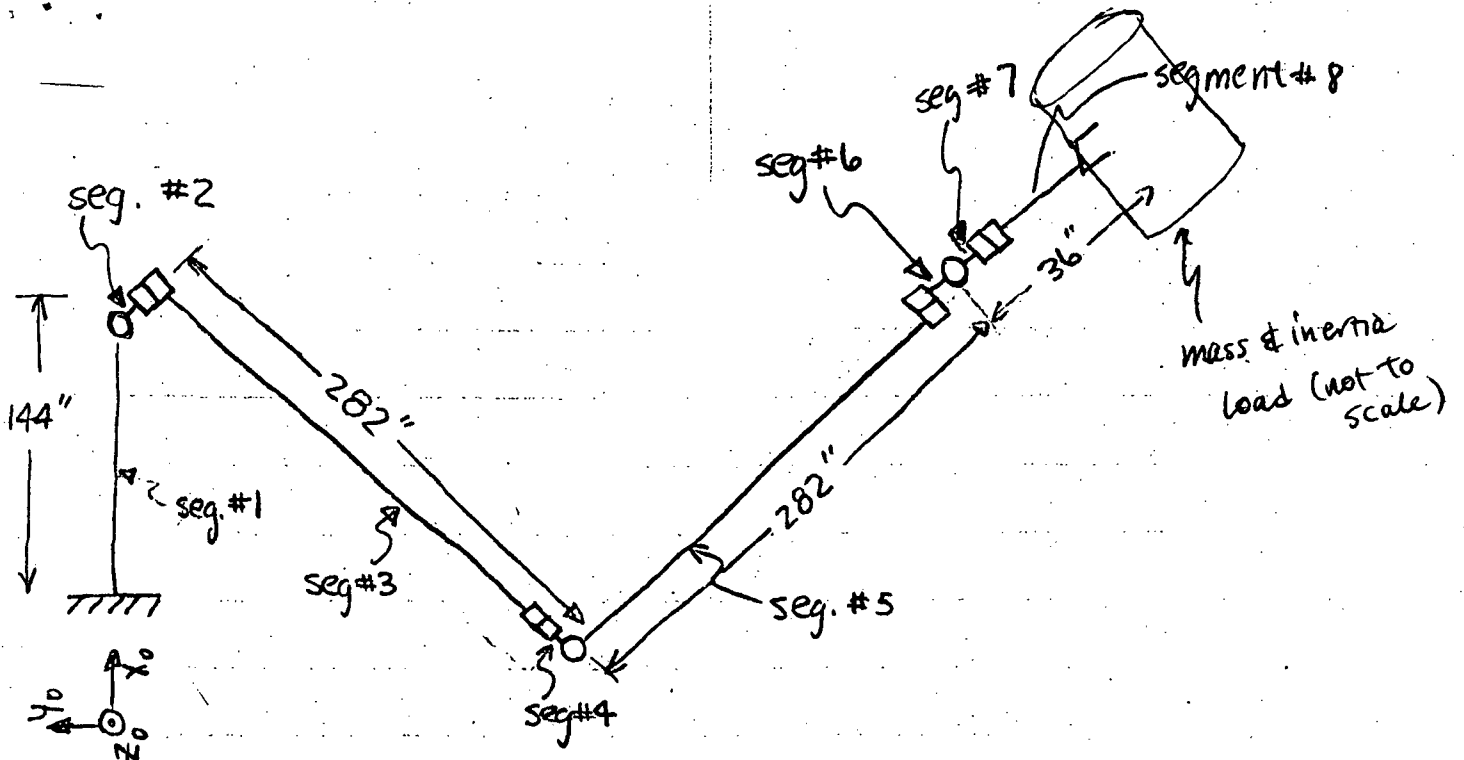


Fig. 7 An arm modeled with more than one lumped mass.



mass = 65,000 lb_m

$I_{zz} = 8.55 \times 10^8$ lb_m in²

(a solid cylinder $r = 150''$
 $l = 300''$)

Fig. 8 Example arm configuration.

Legend
 Curve 1: Δx (in.)
 Curve 2: Δy (in.)
 Curve 3: $\Delta \theta_z$ (rad $\times 10^2$)

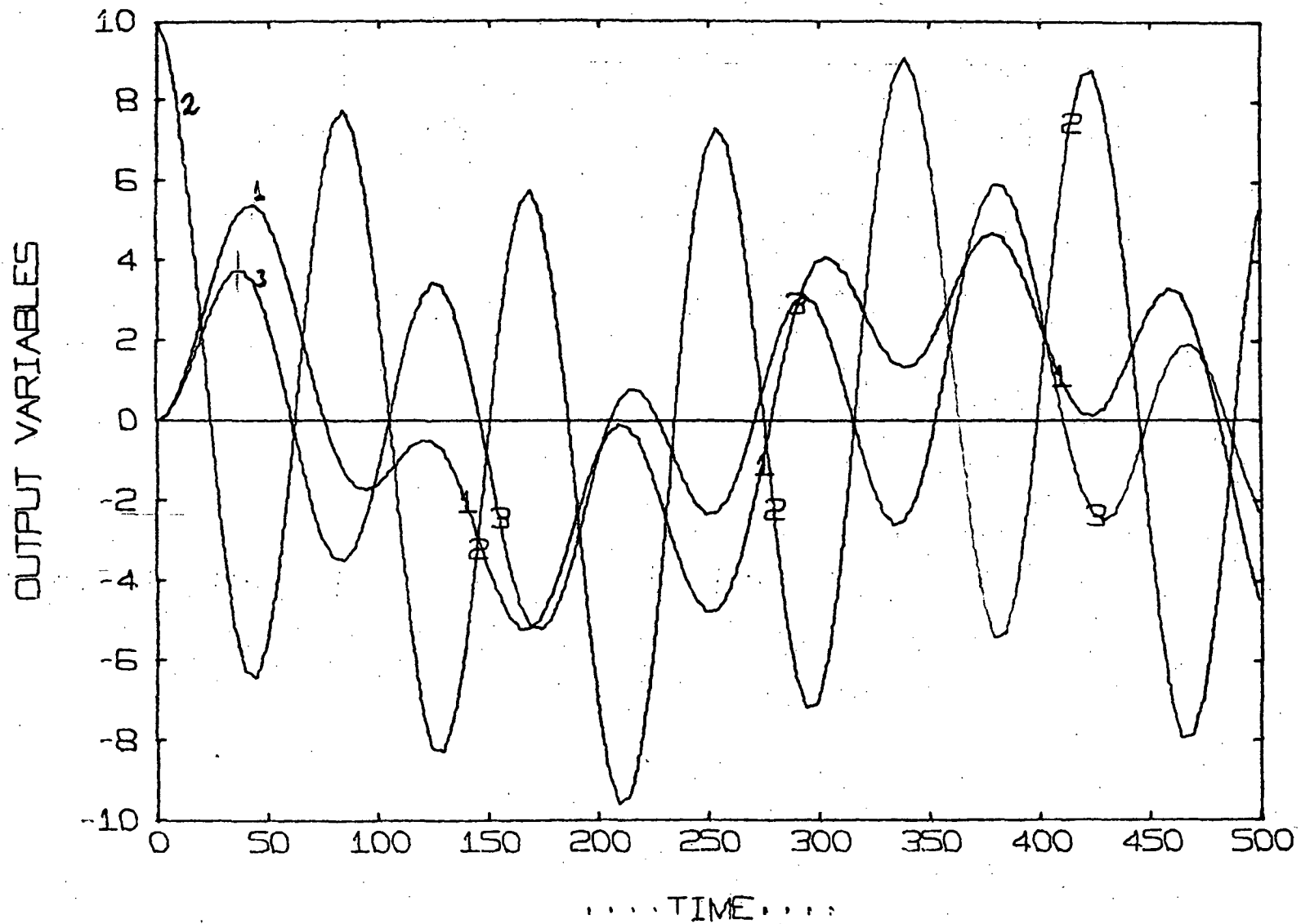


Figure 9. Time response of example.

TABLE 1 ARM PARAMETERS for Example Problem.

i	α_{ci} AC(I)	α_{xfi} AXF(I)	α_{xmi} AXM(I)	$\alpha_{\theta fi}$ ATM(I)	α_{Ti} AT(I)
1	7.7000E-07	2.9300E-04	3.0500E-06	4.2500E-08	5.3100E-08
2	0.0000E 00	0.0000E 00	0.0000E 00	0.0000E 00	0.0000E 00
3	1.4400E-06	4.7500E-03	2.5200E-05	1.7900E-07	1.2500E-07
4	0.0000E 00	0.0000E 00	0.0000E 00	0.0000E 00	0.0000E 00
5	3.6200E-06	1.1900E-02	6.3700E-05	4.5000E-07	5.6500E-07
6	0.0000E 00	0.0000E 00	0.0000E 00	0.0000E 00	0.0000E 00
7	0.0000E 00	0.0000E 00	0.0000E 00	0.0000E 00	0.0000E 00
8	9.2400E-07	1.9900E-04	8.3000E-06	4.6000E-07	5.7700E-07
	(in./lb _f)	(in./lb _f)	(in./in.-lb _f)	(rad./in.-lb _f)	(rad./in lb _f)

COURIER-UNIFORM-1

$$\alpha_{\theta fi} (\text{rad./lb}_f) = \alpha_{xmi} (\text{in./in.-lb}_f)$$

Real time trajectory generation

Introduction

Subject of the investigations is a planar three joint arm with joint angles θ_1 , θ_2 and θ_3 as shown in figure 1.

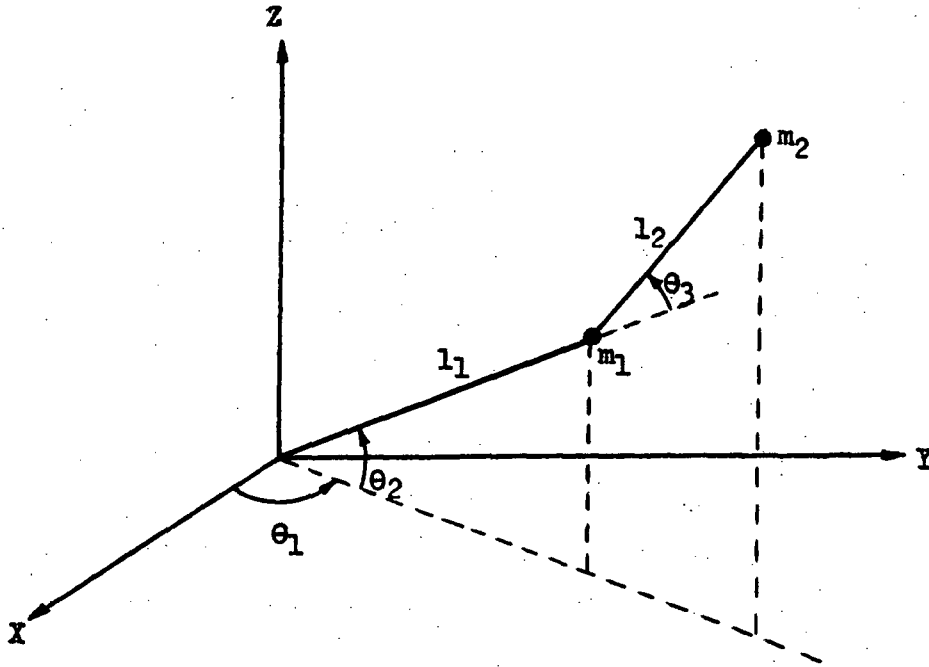


Figure 1.

To move the arm from an initial position $\theta_i = [\theta_{1i}, \theta_{2i}, \theta_{3i}]$ to a final position $\theta_f = [\theta_{1f}, \theta_{2f}, \theta_{3f}]$ in T seconds it is necessary that a trajectory in θ -space is generated in T seconds. It is required that the trajectory is such that a given performance criterion is satisfied; i. e., a given cost function J must be minimum over the path between the prescribed end points. The optimal trajectories are obtained as follows:

Assume that the time function for each joint angle θ_k ($k = 1, 2, 3$) can be written as a series of elementary functions

$$\theta_k = f_0(t) + A_k f_1(t) + B_k f_2(t) + \dots \quad (1)$$

$$k = 1, 2, 3$$

where A_k, B_k, \dots are time-invariant parameters.

Generally, for a specific arm the cost function J is a function of

$\theta_k, \dot{\theta}_k, \ddot{\theta}_k$ and T .

Substituting the assumed functions for $\theta_k, \dot{\theta}_k$ and $\ddot{\theta}_k$ in the expression for J , J can be written as a function of the parameters

A_k, B_k, \dots , the initial and final angles θ_{ki} and θ_{kf} , and T .

If θ_{ki}, θ_{kf} and T are prescribed J is only a function of A_k, B_k, \dots

The values of A_k, B_k, \dots for which J is minimum can be obtained by numerical search.

State of the work at the beginning of the quarter

At this time computer programs to find the optimal values of the parameters A_k, B_k, \dots for different cost functions J and different kinds of trajectories has been developed and some examples had been worked out.

The cost functions are:

1. The integral between $t = 0$ and $t = T$ of the kinetic energy of the arm:

$$J = \int_0^T KE \, dt \quad (2)$$

2. The integral between $t = 0$ and $t = T$ of the sum of the absolute values of the joint torques:

$$J = \int_0^T \sum_{k=1}^3 |u_k| \, dt \quad (3)$$

The assumed functions for each joint angle θ_k ($k = 1, 2, 3$) are:

- a. A series of polynomials

$$\begin{aligned} \theta_k &= \theta_{ki} + (\theta_{kf} - \theta_{ki}) \frac{t}{T} \\ &+ A_k \frac{4}{T^2} t (T-t) + B_k \frac{64}{T^3} t \left(\frac{T}{2} - t\right) (T-t) \end{aligned} \quad (4)$$

where $\theta_{ki} = \theta_k$ at $t = 0$

$\theta_{kf} = \theta_k$ at $t = T$

The elementary functions are shown in figure 2.

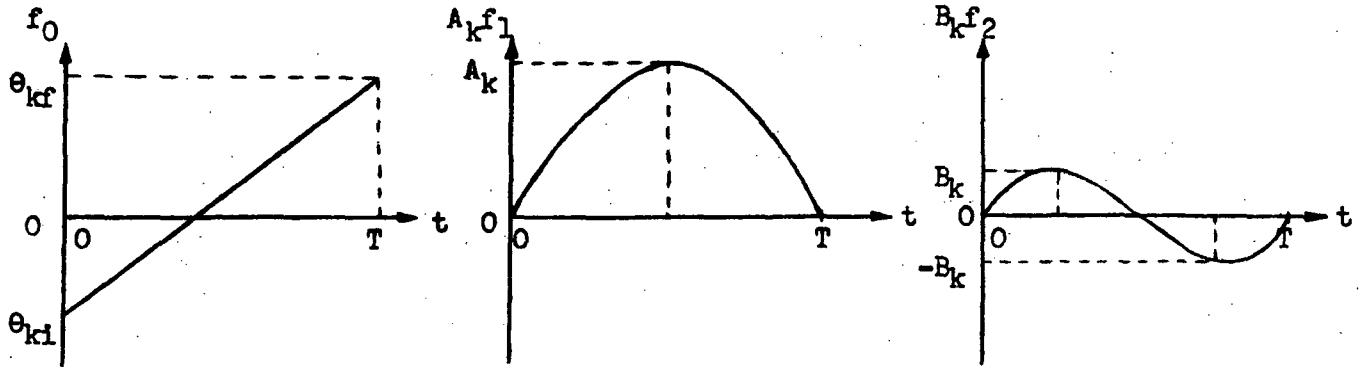


Figure 2.

b. A series of the following three elementary functions, which are periodic:

$$f_0(t) = \theta_{ki} + \frac{\theta_{kf} - \theta_{ki}}{T} \left(t - \frac{1}{\omega} \sin \omega t \right) \quad (5a)$$

$$A_k f_1(t) = \begin{cases} A_k \frac{2}{T} \left(t - \frac{1}{2\omega} \sin 2\omega t \right), & 0 \leq t \leq \frac{T}{2} \\ A_k \left(2 - \frac{2}{T} \left(t - \frac{1}{2\omega} \sin 2\omega t \right) \right), & \frac{T}{2} \leq t \leq T \end{cases} \quad (5b)$$

$$B_k f_2(t) = \begin{cases} B_k \frac{4}{T} \left(t - \frac{1}{4\omega} \sin 4\omega t \right), & 0 \leq t \leq \frac{T}{4} \\ B_k \left(2 - \frac{4}{T} \left(t - \frac{1}{4\omega} \sin 4\omega t \right) \right), & \frac{T}{4} \leq t \leq \frac{3T}{4} \\ B_k \left(-4 + \frac{4}{T} \left(t - \frac{1}{4\omega} \sin 4\omega t \right) \right), & \frac{3T}{4} \leq t \leq T \end{cases} \quad (5c)$$

where $\omega = 2\pi/T$

Figure 3 shows these functions

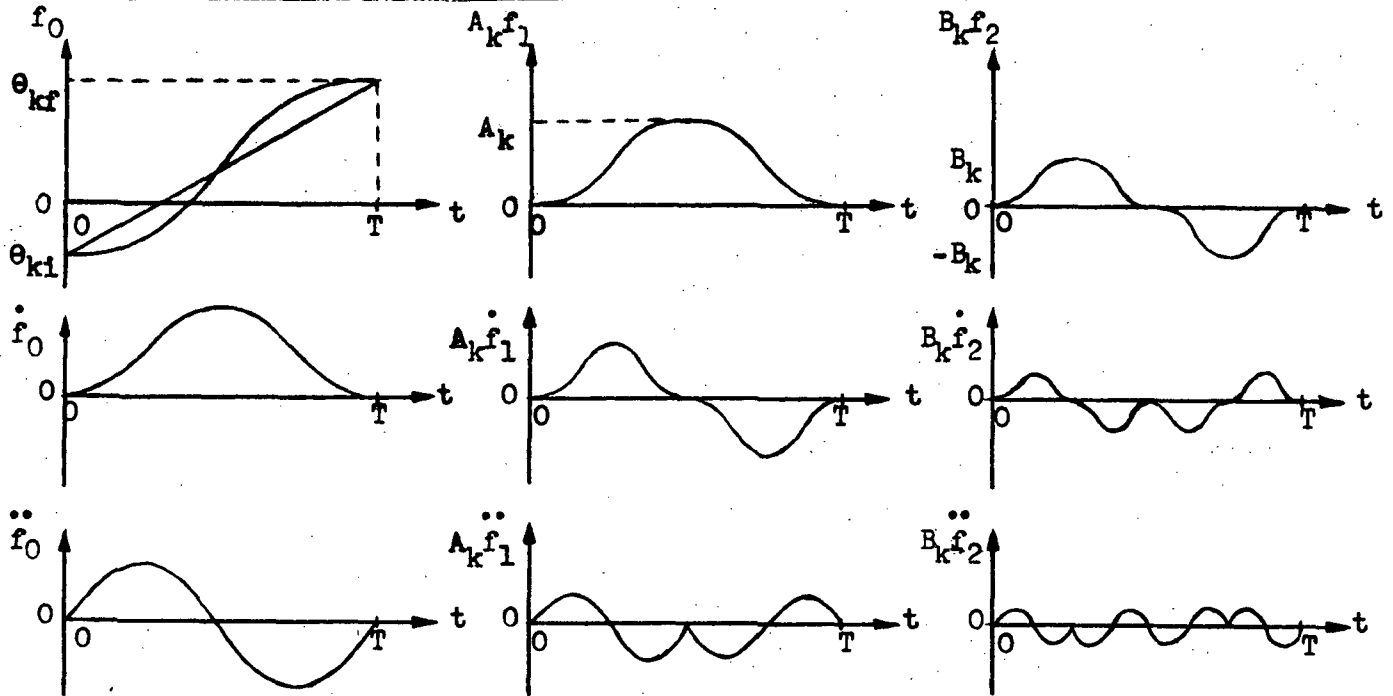


Figure 3.

With the programs the optimal values of A_k and B_k could be obtained for the following combinations of cost function and trajectory:

- I. $J = \int_0^T KE \, dt$ with trajectory (4), a series of polynomials
- II. $J = \int_0^T KE \, dt$ with trajectory (5), a series of periodic functions.
- III. $J = \int_0^T \sum_{k=1}^3 |u_k| \, dt$ with trajectory (5).

Combination of $J = \int_0^T \sum_{k=1}^3 |u_k| \, dt$ with trajectory (4) is not possible. The joint torques are functions of θ_k , $\dot{\theta}_k$ and $\ddot{\theta}_k$. For trajectory (4) $\ddot{\theta}_k$ is infinite at $t = 0$ and $t = T$.

Work performed during this quarter

For the evaluation of the cost function J the integral is computed with Simpson's rule. A problem was the choice of the number of intervals in between $t = 0$ and $t = T$, which will be determined by:

- nature of the integrand
- required accuracy in the parameters A_k and B_k .

- cost of computer time (for each evaluation of J the integrand must be computed n + 1 times)

Satisfactory results were obtained by choosing n = 20.

For a specific arm ($l_1 = l_2 = 0.3$ m and $m_1 = m_2 = 1$ kg) the three programs have been run for over 20 combinations of initial and final positions of the arm.

In all cases $T = 2$, $\theta_{1i} = -0.78$ and $\theta_{1f} = +0.78$; θ_{2i} and θ_{2f} vary between -1.57 and $+0.78$; and θ_{3i} and θ_{3f} vary between 0.0 and 2.36 (angles in radians).

The following results for the optimal values of A_k and B_k were obtained.

I. $J = \int_0^T KE dt$ for trajectory (4)

For all combinations of θ_i and θ_f B_1, B_2 and B_3 are 0.

When both $\theta_{2i} = \theta_{2f}$ and $\theta_{3i} = \theta_{3f}$ $A_1 = 0$ too.

For these cases A_2 and A_3 have been plotted as functions of $\theta_{2i} = \theta_{2f} = \theta_2$ and $\theta_{3i} = \theta_{3f} = \theta_3$ (figure 4)

In most other cases ($\theta_{2i} \neq \theta_{2f}$ and/or $\theta_{3i} \neq \theta_{3f}$) A_1 has a nonzero value.

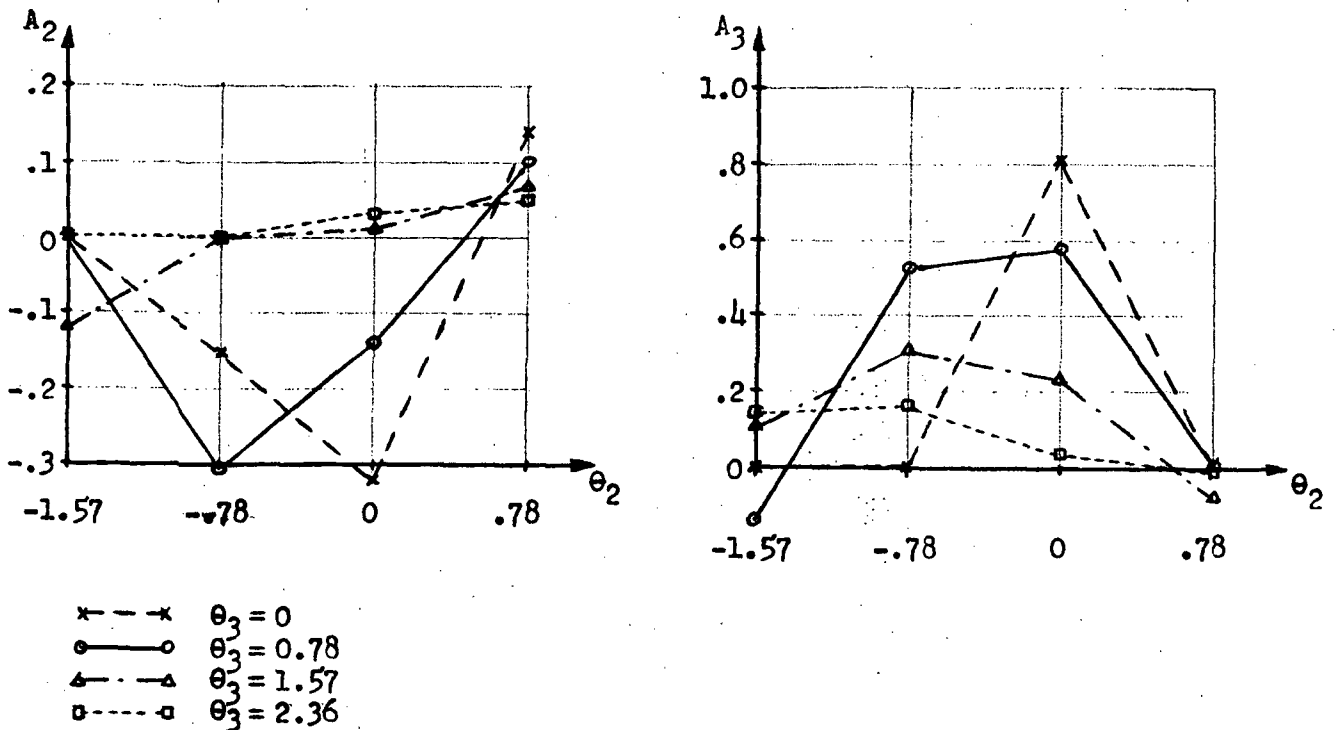


Figure 4.

II. $J = \int_0^T KE dt$ for trajectory (5)

For $\theta_{2i} = \theta_{2f}$ and $\theta_{3i} = \theta_{3f}$ the optimal values of A_2 , B_2 and B_3 are 0, while B_1 has values between 0.11 and 0.18.

The values of A_2 and A_3 are shown in figure 5.

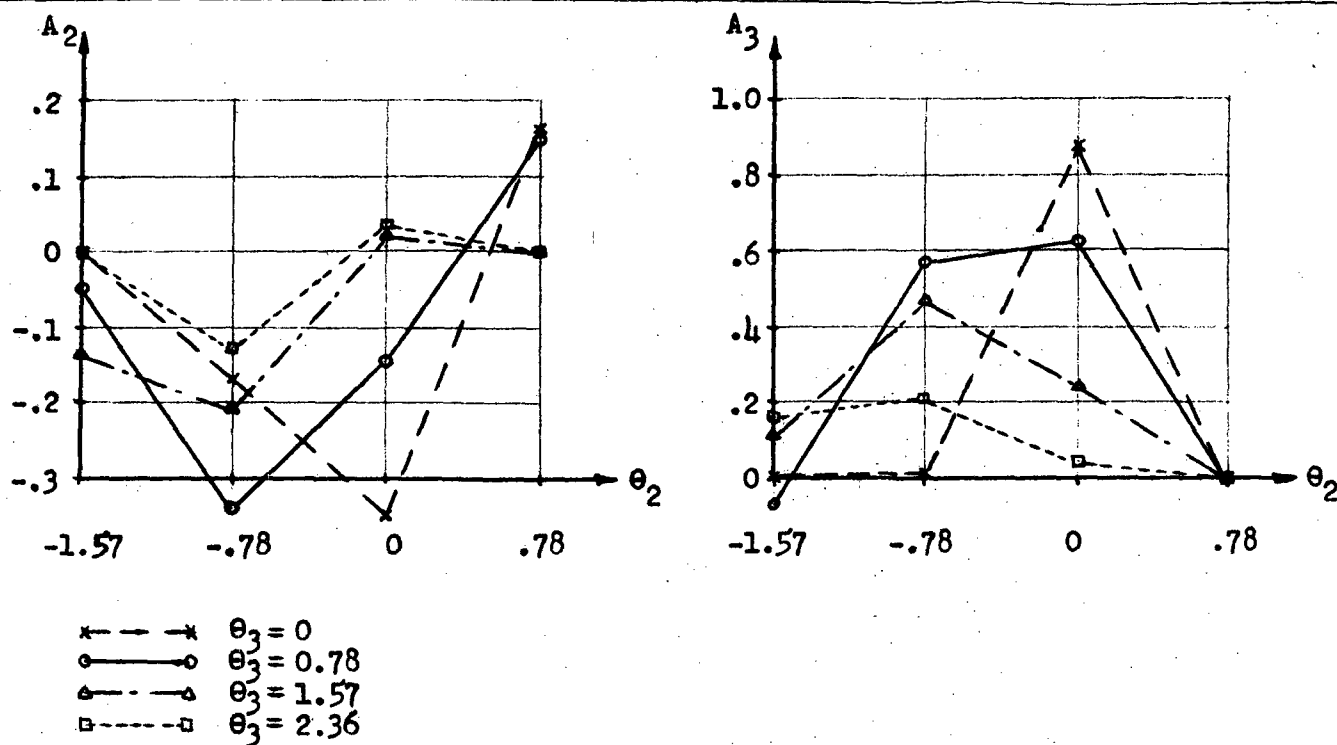


Figure 5.

III. $J = \int_0^T \sum_{k=1}^3 |u_k| dt$ for trajectory (5)

As in I the optimal values of A_1 , B_1 , B_2 are 0 when both $\theta_{2i} = \theta_{2f}$ and $\theta_{3i} = \theta_{3f}$. In figure 6 the values of A_2 and A_3 are plotted for these cases.

For $\theta_{2i} \neq \theta_{2f}$ and/or $\theta_{3i} \neq \theta_{3f}$ parameter A_1 has a value $\neq 0$.

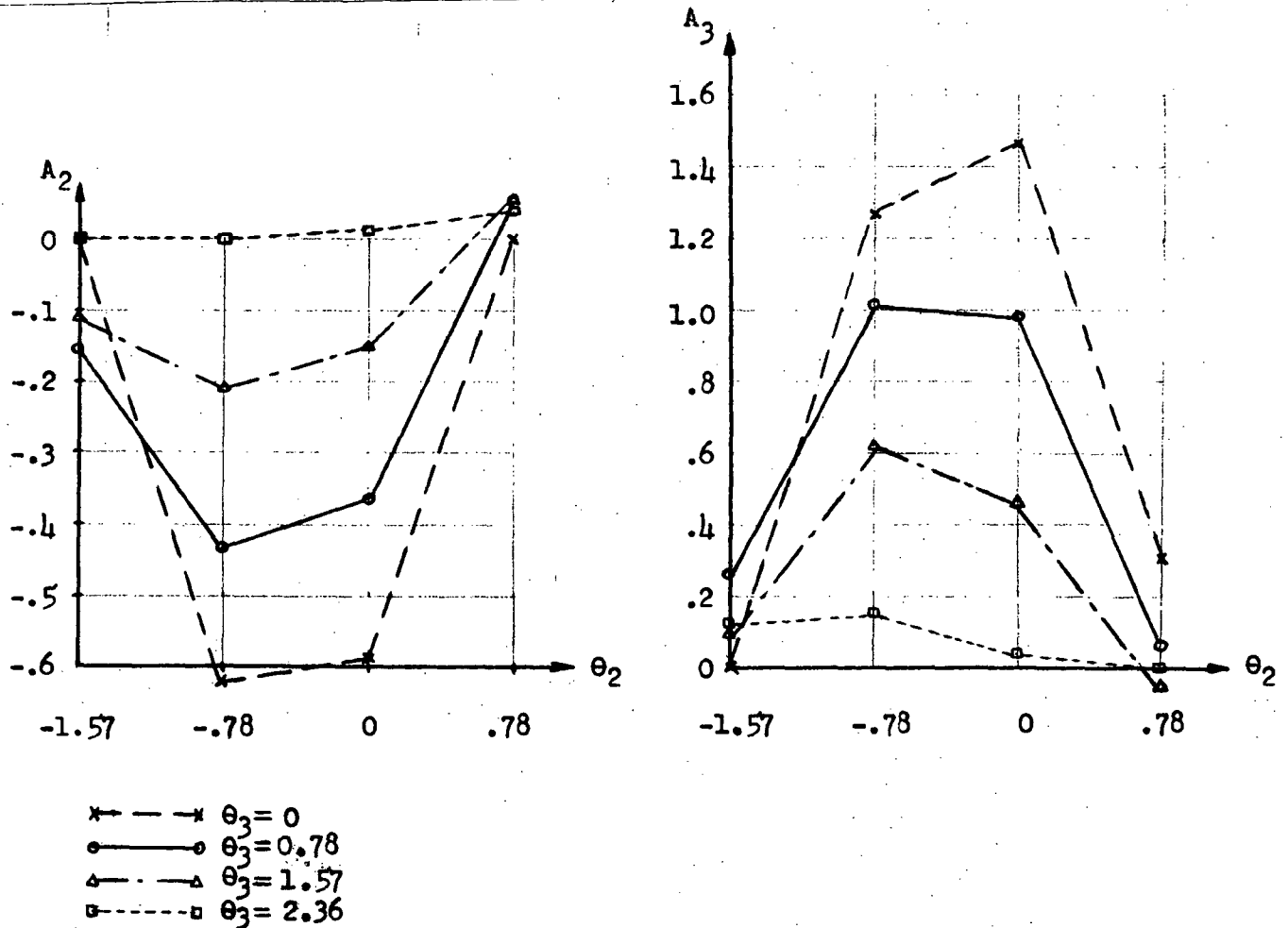


Figure 6.

Considering the values of the cost function in the different cases the following comments can be made;

1. The value of $\int_0^T \sum_{k=1}^3 |u_k| dt$ seems to be more sensitive to variations in the values of the parameters A_k and B_k than $\int_0^T KE dt$.
2. In case III the minimum values of J are at most 35% lower than the values of J with all parameters A_k and B_k equal to zero. This is an indication that the trajectory with all A_k and B_k equal to zero is rather good for this cost function.
3. The value of $J = \int_0^T KE dt$ for trajectory (4) (series of polynomials) is lower than for trajectory (5) (series of periodic functions).

Furthermore attention has been paid to the problem of fitting curves through results shown in figure 4, 5 and 6. For example, for figure 6

(case III) parabolas were fitted through each set of 4 points with the same θ_3 . These parabolas went through $(-1.57, 0)$ and $(+0.78, 0)$ with the top on the line $\theta_2 = -0.3925$ ($= -\frac{\pi}{8}$). Assuming that for a particular θ_2 the values of the parameters A_2 and A_3 vary linearly with θ_3 , it was possible to summarize the results for A_2 and A_3 in two simple expressions. In most cases the value of the cost function computed with these sub-optimal values of A_2 and A_3 was 0 - 20% bigger than the minimum value. However for a couple of points the difference with the minimum was 40 - 50%.

Although there is a pattern in the results for case II and III (figure 4 and 5) it is not obvious which kind of function would give the best fit.

Future Work

For the time to come work on the following points has been planned:

1. Analysis of the sensitivity of the parameters A_k and B_k to the values of θ_2 and θ_3 .
2. Improvement of the suboptimal results using curves which give a better fit to the optimal results; this also for cases in which $\theta_{2i} \neq \theta_{2f}$ and/or $\theta_{3i} \neq \theta_{3f}$.
3. Writing a thesis about the work performed since September 1971.

The Effect of Visual Feedback on Remote Manipulator Performance

This study concerns remote manipulators which are controlled by human operators (as opposed to automated devices). It is assumed that in order for the man-manipulator system to perform a task, some visual feedback of the work area is needed. We are interested in determining the effects on operator performance when various types of visual feedback are employed: specifically, what effect a closed circuit television system will have on manipulator performance, and how such a system should be arranged so as to yield the best performance.

The tasks which were to be performed involved placing a $3/4$ " diameter four inch long rod into three holes each one inch in diameter, and two inches deep. Three electric stopwatches were connected to switches at the bottoms of the holes, so that the time intervals required to move from one hole to the next could be measured.

Two orientations of hole direction were employed - one in which all the centerlines were parallel (task A, see figure 1-A) and the second in which all centerlines met at angles of 120° (Task B, see figure 1-B). Both of these tasks were run with the plane of the blocks parallel to, and inclined 30° to, the floor (see figure 2).

One form of manipulation has been tested so far - master-slave using a mechanical AMF manipulator. This device has six degrees of freedom, with 1:1 position control between master and slave. Three types of video feedback have been tested - direct viewing, closed circuit T.V. with the camera fixed along the sight axis of direct viewing, and closed circuit with the camera fixed to the manipulator (see figure 3)

The procedure for running a test with all combinations of task and manipulator was as follows: the peg was initially placed in the right most hole (with respect to the operator) and all clocks were initialized. The subject was then to move the peg counterclockwise around the "triangle" of holes, finishing when it was back in the first hole. The times were recorded for each interval, and the procedure repeated. Ten runs were made for each combination of task, and video system.

The average of each of the three intervals was taken for each combination over all ten runs, as well as over the last five runs. This

procedure was followed because it was observed that the reduction in task completion time due to learning took place largely in the first five runs. These averages are listed in table 1.

By averaging the three intervals for each situation, a single indication of system efficiency can be produced. These averages are shown in table 2-A. Taking the ratio of fixed camera and moving camera average times to direct viewing times for each task, a relative comparison can be made between the methods of visual feedback. These results are shown in table 2-B.

Some observations were made concerning each system, which serve to explain some of the numerical findings:

In all cases the force feedback inherent to the AMF mechanically coupled manipulator served to augment the operator's knowledge. Although in task B, the third hole is not clearly visible with the direct or fixed camera systems, the force feedback allows the operator to find the hole quite easily, once the gross alignment has been performed visually.

The repeatability of the motions involved in each of the tasks, as well as the one to one nature of the manipulator, allowed the operator to adapt to a new task quite quickly. After the initial few runs, his memory of where and how far to move the master arm served to facilitate the gross positioning of the peg. This factor would not be present in an unrehearsed task.

When performing either task with the plane of the blocks inclined 30° , the time interval required to go from hole #2 to hole #3 was frequently lower than the other two intervals generated. This was because these two holes were at the same vertical level, and as a result, required one fewer degree of freedom to be oriented. This phenomenon was especially noticeable for task A, inclined, with the camera mounted on the manipulator arm. With this camera position, vertical distance cannot be seen directly; hence the maneuver which require the least vertical alignment was easiest to perform. The B-C time was not the lowest for task B, inclined, because the camera orientation did not allow viewing behind the manipulator arm; i. e. where block #C was located.

With the camera mounted to the manipulator arm, a rotation of the camera about its viewing axis was possible. As long as the arm was held so that the camera to task alignment shown in figure 4 was retained, the operator did not lose his orientation. The wrist could rotate independent

of the arm rotation, so that holding the arm to preserve the camera angle was no penalty. However, once the camera was rotated from the alignment shown in figure 4, it became difficult to decide what direction of control motion would produce the desired effect.

These are the tests and results which have been conducted in this area to date. Future tests will evaluate the effect of visual feedback on resolved rate manipulation, as well as the merits of resolved rate camera manipulation as compared to the "moving window" system. It is also of interest to see how the resolved rate system will perform with the frame of reference of the T.V. camera fixed to the hand, since all motions are carried out in hand coordinates for this system.

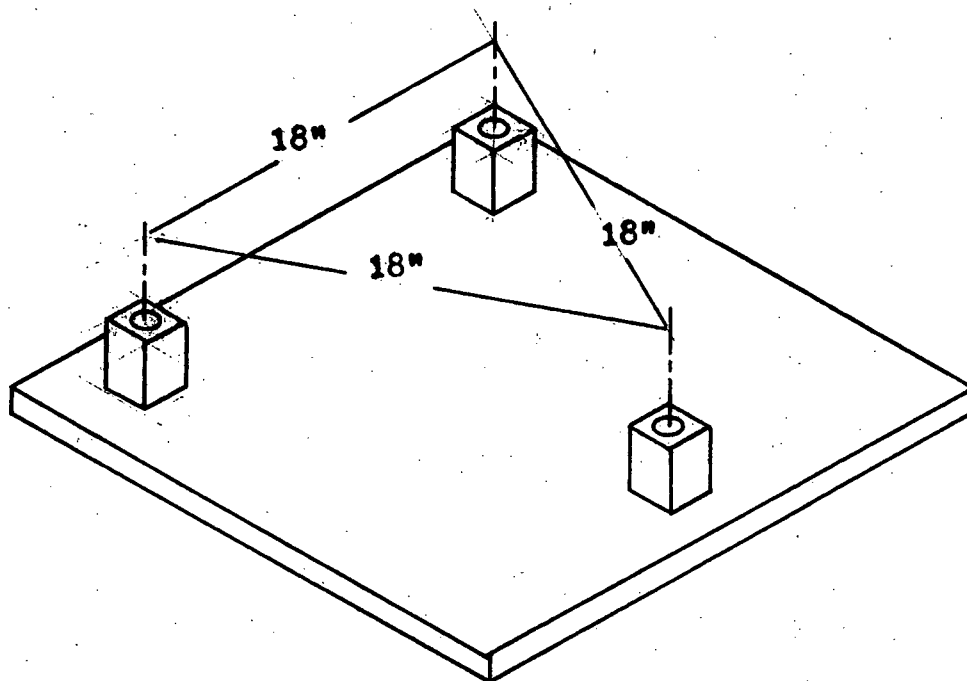


FIGURE 1-A TASK A

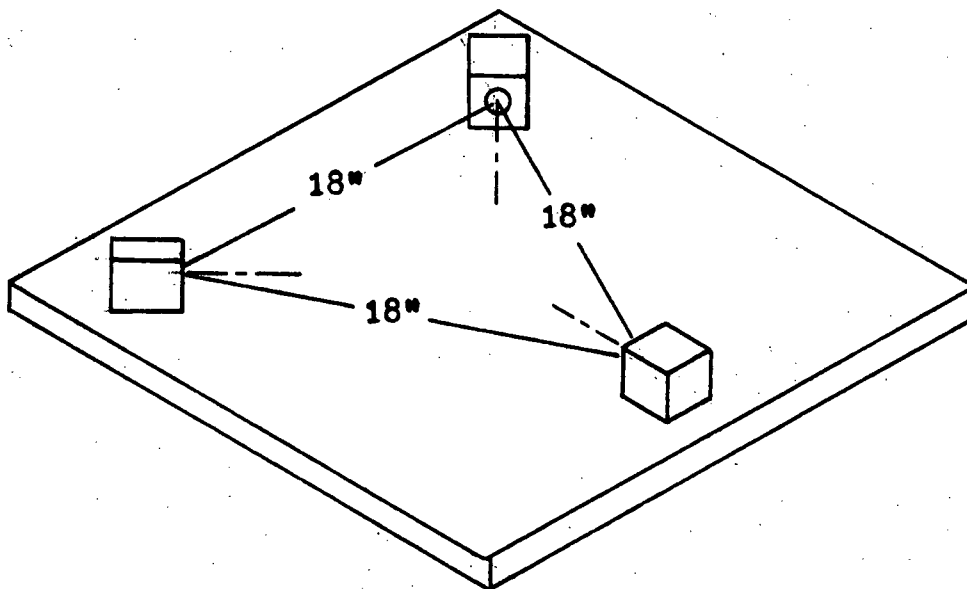
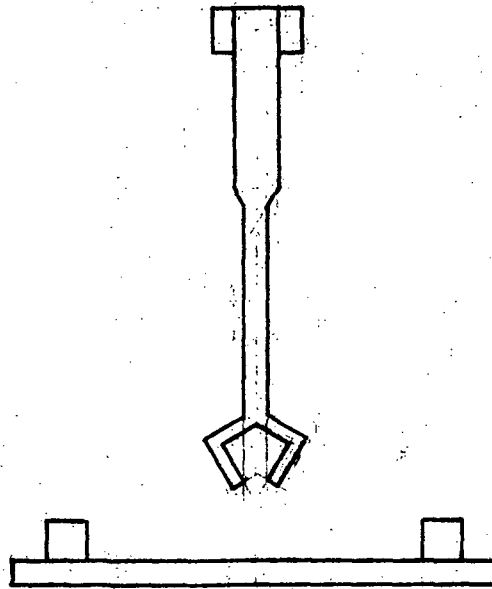
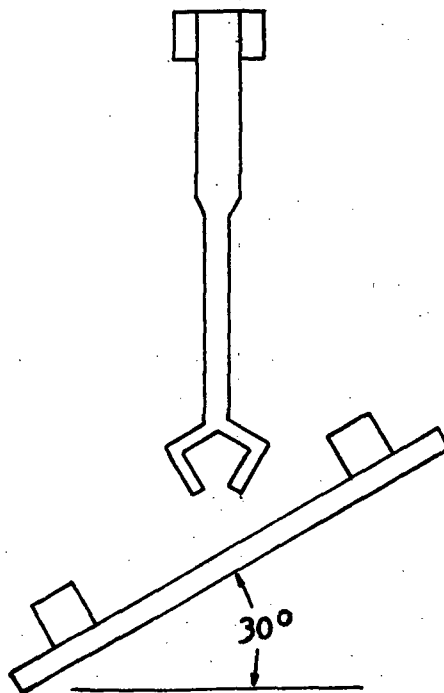


FIGURE 1-B TASK B



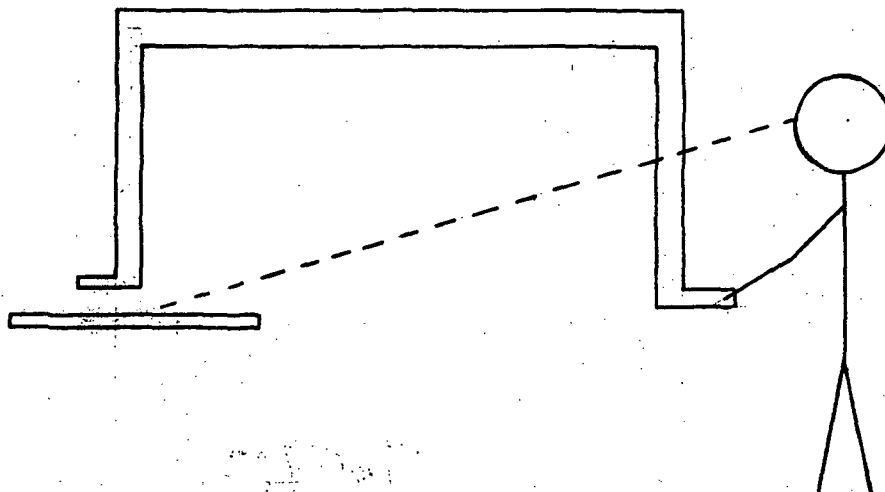
TASK PARALLEL TO FLOOR



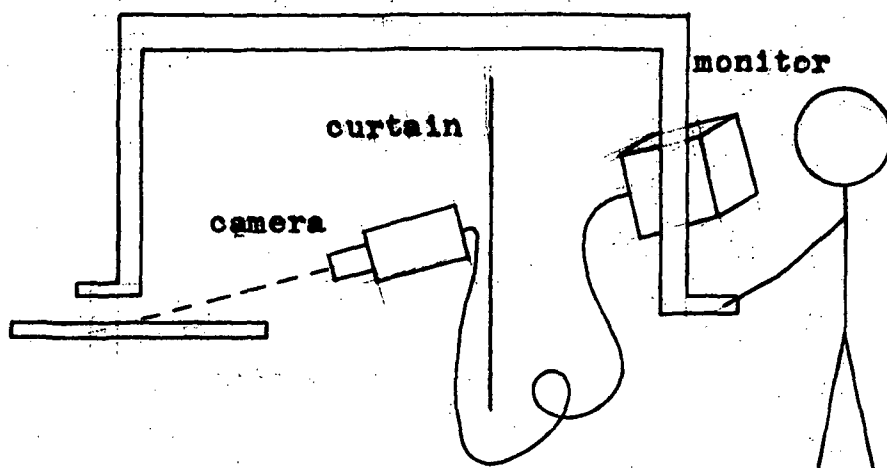
TASK AT 30° INCLINATION

FIGURE 2

DIRECT VIEWING



CLOSED CIRCUIT, CAMERA ALONG SIGHT AXIS



CLOSED CIRCUIT, CAMERA ON MANIPULATOR

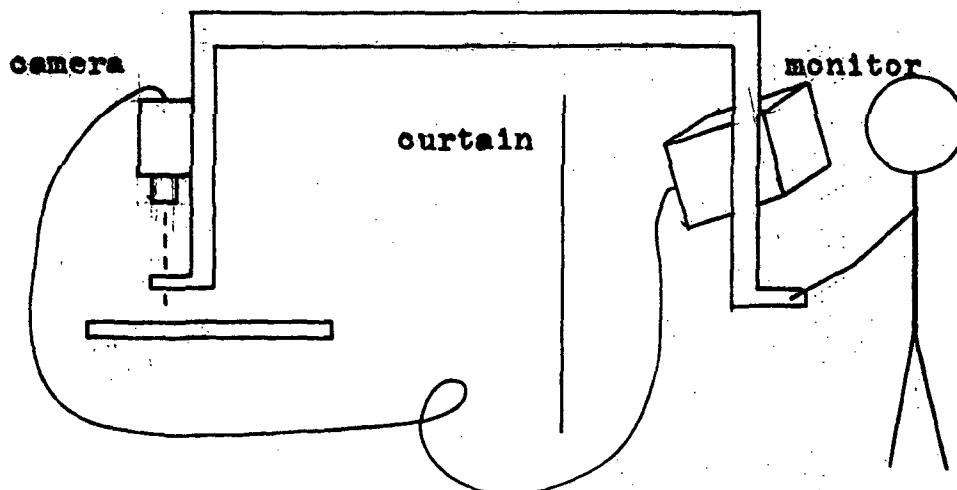
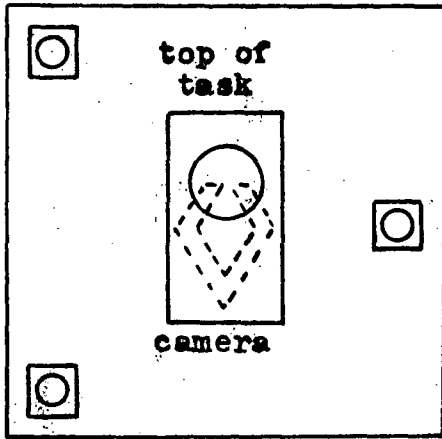
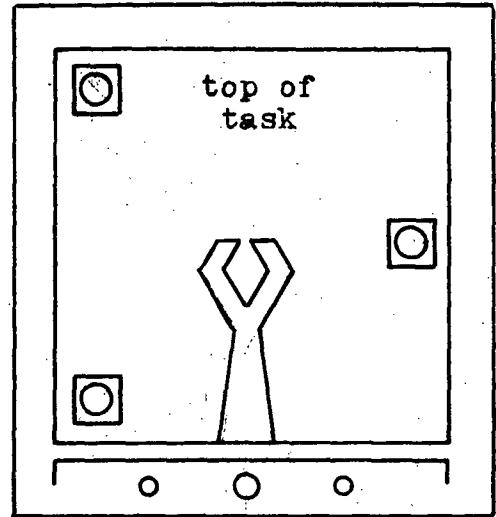


FIGURE 3

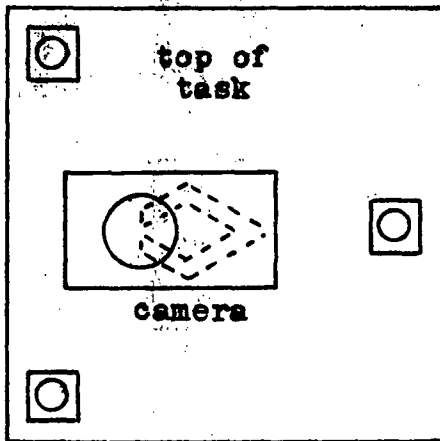


TASK

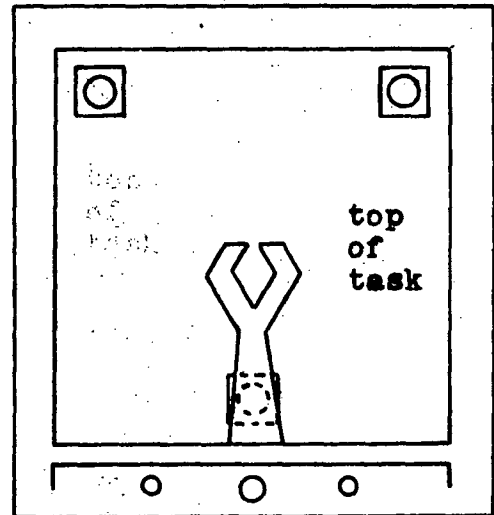


MONITOR

Camera orientation which provided the most useful image



TASK



MONITOR

Camera orientation which provided a confusing image

FIGURE 4 Clarifying and Confusing Image Orientations

DIRECT VIEWING

	A-B	B-C	C-A
TASK A, FLAT	2.34	1.95	2.62
" " 30°	2.66	2.31	2.77
TASK B, FLAT	2.93	2.56	3.04
" " 30°	3.38	3.09	3.25

CLOSED CIRCUIT, FIXED CAMERA

	A-B	B-C	C-A
TASK A, FLAT	6.10	5.04	4.97
" " 30°	6.17	4.24	4.44
TASK B, FLAT	6.10	4.98	4.39
" " 30°	5.87	5.69	5.39

CLOSED CIRCUIT, CAMERA ON MANIPULATOR

	A-B	B-C	C-A
TASK A, FLAT	2.96	2.70	2.74
" " 30°	3.46	2.42	3.84
TASK B, FLAT	3.82	3.61	3.36
" " 30°	6.20	8.40	6.16

TABLE #1

Average task completion times (seconds)

(Averages taken over the final five trials to eliminate the effects of learning)

	DIRECT VIEWING	FIXED CAMERA	MOVING CAMERA
TASK A. FLAT	2.30	5.35	2.80
" " 30°	2.58	6.88	3.24
TASK B. FLAT	2.84	5.15	3.59
" " 30°	3.24	5.65	6.90

TABLE 2-A Average times for each task, with individual moves averaged together.

	FIXED CAMERA	MOVING CAMERA
TASK A. FLAT	2.32	1.22
" " 30°	2.66	1.26
TASK B. FLAT	1.81	1.26
" " 30°	1.74	2.12

TABLE 2-B Ratio of average fixed camera times/ direct viewing times and of moving camera times/ direct viewing times.